2009 American Control Conference
Hyatt Regency Riverfront, St. Louis, MO, USA
June 10-12, 2009

Position-Based Visual Servo Control of Leader-Follower Formation Using Image-Based Relative Pose and Relative Velocity Estimation

A. P. Dani, N. Gans, and W. E. Dixon

***Abstract*— A position-based visual servo control strategy is proposed for leader-follower formation control of unmanned ground vehicles (UGVs). The proposed control law only requires the knowledge of a single known length on the leader. The relative pose and the relative velocity of the leader are estimated with respect to the follower in the follower reference frame. The relative pose and the relative velocity are obtained using a geometric pose estimation technique and a nonlinear velocity estimation strategy, respectively. A Lyapunov analysis indicates global asymptotic tracking of the leader vehicle, and simulation results are provided to illustrate the performance of the developed controller.**

I. INTRODUCTION

Formation control of nonholonomic unmanned guided vehicles (UGV's) has been a topic of extensive research [1]–[4]. Various strategies have been applied for formation control of a group of UGV's, including leader-follower techniques, behaviour-based methods [5], [6] and virtual structure techniques [7]. In the leader-follower approach, one of the UGV's is considered as leader and other UGV's track the position and the orientation of the leader with prescribed offsets [8]–[10].

Vision-based control methods have been applied to the leader-follower problem in a variety of ways (cf. [11]–[15]). These methods can generally be grouped as image-based visual servo control (IBVS) and position-based visual servo control (PBVS). IBVS methods [16], [17], use image features as the state in control laws to regulate the camera to a desired goal pose, which is usually defined as a goal image (i.e. an image captured at a predefined goal pose). The PBVS method [16], [18], uses three dimensional scene information that is reconstructed from image information to regulate the camera motion to a desired pose. Some pose reconstruction methods [19], [20] can be used in PBVS, but require knowledge of the depth to the target in at least one reference image. Other pose reconstruction methods [21] provide depth to the target, but require a model of the target. Recently, some methods have been developed [22]–[24] to reconstruct the pose of an object and velocity of the object with respect to camera using the knowledge of a single length on the object. These methods can be applied in the design of a PBVS leader-follower formation controller for nonholonomic UGV's.

This paper focuses on vision-based formation control of UGV's using the leader-follower approach. The proposed controller uses a recently developed vision-based algorithm to estimate the relative pose of the leader in the camera field of view given a single known length [22]. The relative velocity of the leader is estimated using the nonlinear estimator proposed in [23] and used in the control development to provide more knowledge about the motion of the leader. The developed decentralized controller eliminates the need for any communication between the agents by using relative image information instead of the position and the velocity of the leader in the global reference frame.

The pose and velocity estimation methods in this paper utilize the Euclidean Homography that exists between pairs of images [20], but returns estimates of a targets pose and velocity relative to the camera. In [13], [14], the Euclidean Homography is successfully used in leader-follower control, but the goal pose of the follower must be defined by an a priori goal image. The method in [14], does not include an estimate of the relative velocity of the leader. Omnidirectional vision-based formation control is developed in [12] where optic flow measurements are used for position estimation. The controller developed in [25] estimates the leader velocity using an extended Kalman filter (EKF). The EKF is blended with a neural network (NN) in [15] to provide robustness to unmodeled and unknown dynamics while estimating the motion of the leader. In [26], the velocity of the leader is estimated using a high gain observer (HGO). Stability of these methods is generally limited to ultimately bounded stability, since convergence of the velocity estimate can only be guaranteed to within an arbitrary bound using EKF, NN or HGO. The leader-follower method in this paper uses a nonlinear estimator [23] that is guaranteed to converge to the correct signal, so asymptotic stability can be achieved.

II. BACKGROUND

A. UGV Model

For small steering angles, the kinematic equations of motion for the nonholonomic UGV are assumed to have the following form [27]:

$$\begin{bmatrix} \dot{x}_{ci} \\ \dot{z}_{ci} \end{bmatrix} = \begin{bmatrix} \cos\varphi_i & -\sin\varphi_i \\ \sin\varphi_i & \cos\varphi_i \end{bmatrix} \begin{bmatrix} v_i \\ \omega_i \end{bmatrix},$$
$$\dot{\varphi}_i = \omega_i \tag{1}$$

where $(x_{ci}(t), z_{ci}(t)) \in \mathbb{R}^2$ denotes the position of the UGV in a world reference frame, and $\varphi_i(t) \in \mathbb{R}$ is the heading

This research is supported in part by the NSF CAREER award 0547448. The authors would like to acknowledge the support of the Department of Energy, grant number DE-FG04-86NE37967. This work was accomplished as part of the DOE University Research Program in Robotics (URPR).

A. P. Dani and W. E. Dixon are with the Department of Mechanical and Aerospace Engineering, University of Florida, Gainesville, FL 32611-6250, USA. Email: ashwin31@ufl.edu. wdixon@ufl.edu

N. Gans is with the National Research Council and Air Force Research Laboratory, Egline AFB, FL. Email:ngans@ufl.edu

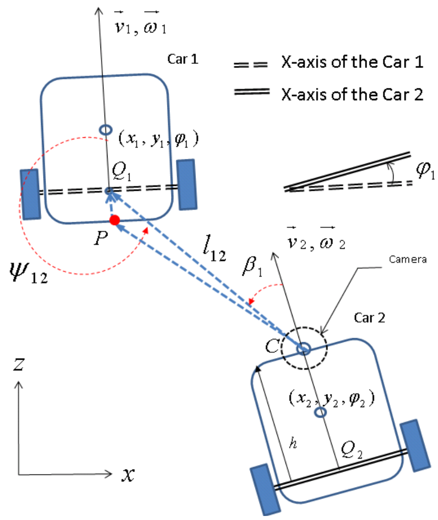

Fig. 1. UGVs in leader-follower formation

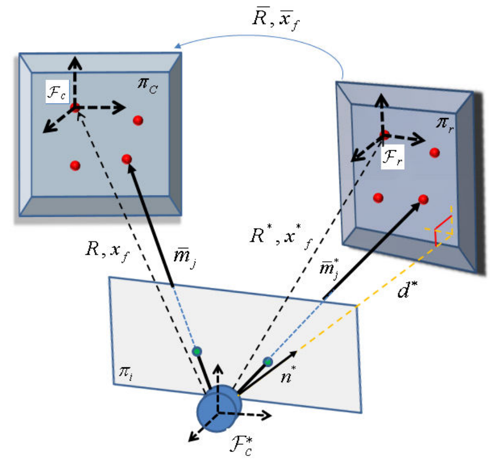

Fig. 2. Coordinate relationship

angle. The vectors $\vec{v}_i(t)$ and $\vec{\omega}_i(t)$ denote the linear and angular velocity of the i^{th} UGV, where $v_i(t)$ and $\omega_i(t)$ denote the magnitudes of $\vec{v}_i(t)$ and $\vec{\omega}_i(t)$ respectively. The distance between driving wheel axis Q_2 to the point C, where camera is mounted, is denoted by h in the $x - z$ plane as shown in Fig. 1. The relative distance between the UGVs is denoted by $l_{12}(t)$ and is measured as the distance between the center of the rear wheel axis of the leader UGV and the camera mounted on the follower UGV. The relative distance $l_{12}(t)$ can be calculated as vector addition of the relative pose of a feature point P on the leader UGV and a known distance between P and Q_1. The relative orientation between two UGVs can be defined as

$$\varphi_{12}(t) \triangleq \varphi_1(t) - \varphi_2(t).$$

The relative bearing between $\vec{v}_2(t)$ and $l_{12}(t)$ is given by

$$\beta_1(t) = \pi - \psi_{12} - \varphi_{12}$$

where $\psi_{12}(t)$ is the angle between $\vec{v}_1(t)$ and vector $l_{12}(t)$ as shown in Fig. 1.

B. Relationships between Image and Euclidean Space

Consider a camera with an attached, orthogonal reference frame $\mathcal{F}^*_c$ as shown in Fig. 2. The camera views four or more planar and non-colinear feature points lying fixed in a visible plane π_r of an object in front of the camera. The 3D coordinates of the feature points expressed in the camera frame $\mathcal{F}^*_c$ are $\bar{m}^*_j \in \mathbb{R}^3$ given as

$$\bar{m}^*_j = [x^*_j, y^*_j, z^*_j]^T, \forall j \in \{j = 1, 2, ..., n\}.$$

These feature points, projected on the image plane π_i, are given by normalized coordinates $m^*_j \in \mathbb{R}^3$ as

$$m^*_j = [\frac{x^*_j}{z^*_j}, \frac{y^*_j}{z^*_j}, 1]^T, \forall j \in \{j = 1, 2, ..., n\}.$$

An orthogonal coordinate frame $\mathcal{F}_r$ is attached to plane π_r. The normal vector to plane π_r, measured in $\mathcal{F}^*_c$, is given by $n^* \in \mathbb{R}^3$. The plane is rotated by $\bar{R}(t) \in SO(3)$ and translated by $\bar{x}(t) \in \mathbb{R}^3$ to a new location denoted as π_c. An orthogonal reference frame, denoted by $\mathcal{F}_c$, is attached to the plane π_c. The rotation between the camera frame $\mathcal{F}^*_c$ and the current object frame $\mathcal{F}_c$ is denoted by $R(t) \in SO(3)$ and the rotation between the camera frame $\mathcal{F}^*_c$ and the reference object frame $\mathcal{F}_r$ is denoted by $R^* \in SO(3)$. The translation vector between $\mathcal{F}^*_c$ and $\mathcal{F}_r$ is given as $x^* \in \mathbb{R}^3$. The feature points in π_c have Euclidean coordinates denoted by $\bar{m}_j(t) \in \mathbb{R}^3$ and normalized Euclidean coordinates $m_j(t) \in \mathbb{R}^3$, measured in camera frame $\mathcal{F}^*_c$, given as

$$\begin{aligned} \bar{m}_j &= [x_j, y_j, z_j]^T, \forall j \in \{j = 1, 2, ..., n\}, \\ m_j &= [\frac{x_j}{z_j}, \frac{y_j}{z_j}, 1]^T, \forall j \in \{j = 1, 2, ..., n\}. \end{aligned}$$

Feature points m^*_j and $m_j(t)$, measured in camera frame $\mathcal{F}^*_c$, are related by a depth ratio $\alpha(t) \in \mathbb{R}$ and the matrix $H(t) \in \mathbb{R}^{3\times 3}$ as

$$m_j = \underbrace{\frac{x^*_{3j}}{x_{3j}}}_{\alpha_j(t)} \underbrace{\left(\bar{R} + \frac{\bar{x}_f}{d^*} n^{*T}\right)}_{H} m^*_j. \tag{2}$$

The Homography matrix can be decomposed to recover the rotation $\bar{R}(t)$ between π_r and π_c, the normal vector n^*, a scaled translation $\frac{\bar{x}(t)}{d^*}$, and depth ratio $\alpha_j(t)$ using standard techniques [28].

Using projective geometry, the normalized coordinates of the feature points in the image plane, m^*_j and $m_j(t)$, are related to the pixel coordinates as

$$p_j = A m_j, \qquad p^*_j = A m^*_j \tag{3}$$

where $A \in \mathbb{R}^{3\times 3}$ is a constant, invertible camera calibration matrix [29]. Using (3), the Euclidean relationship in (2) is given as

$$p_j = \alpha_j A H A^{-1} p^*_j.$$

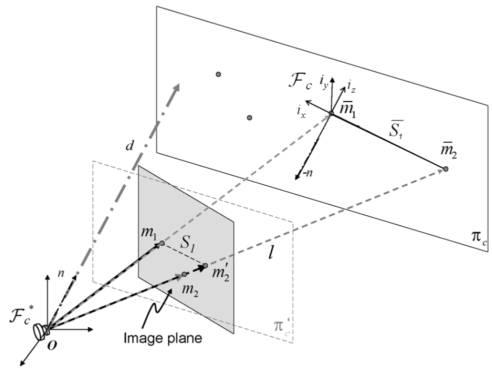

Fig. 3. Reconstruction of a plane with respect to camera

If A is known and at least four feature points are available, a set of linear equations can be solved to get $H(t)$, which can be decomposed into $\bar{R}(t), n^*$, $\frac{\bar{x}(t)}{d^*}$, and $\alpha_j(t)$.

III. Estimation of Relative Pose and Relative Velocity Using a Single Camera

A. Pose Reconstruction using Coplanar Feature Points

An approach, presented in [22], to reconstruct the pose of the frame $\mathcal{F}_c$, attached to the object plane, with respect to the camera frame $\mathcal{F}_c^*$ is described briefly in this section. The pose is calculated using only the knowledge of a single length between $\bar{m}_1$ and $\bar{m}_2$, denoted by $\bar{S}_1$. Using the rotation matrix $\bar{R}(t)$ and normal vector n^* recovered from the homography decomposition, as shown in (2), the normal $n(t)$ to the plane π_c can be determined as

$$n = \bar{R}n^*.$$

Without loss of generality, the origin of the frame $\mathcal{F}_c$ is attached to the feature point $\bar{m}_1(t)$. The orthogonal matrix formed by three axes of $\mathcal{F}_c$ gives the rotation between $\mathcal{F}_c$ and $\mathcal{F}_c^*$ as

$$R = [i_x, i_y, i_z]. \tag{4}$$

If $\bar{m}_1(t)$ and $\bar{m}_2(t)$ are known, i_x and i_y can be calculated as shown in [22]. To determine $\bar{m}_1(t)$ and $\bar{m}_2(t)$, consider a new plane π_c' parallel to plane π_c containing the normalized image point $m_1(t)$. A line l is defined from the origin of $\mathcal{F}_c^*$ through $m_2(t)$ and $\bar{m}_2(t)$. The plane π_c' intersects l at a point $m_2'(t)$. The unknown distance between $m_1(t)$ and $m_2'(t)$ is S_1, as illustrated in Fig. 3.

The point of intersection of the plane π_c' and the line l, denoted by $m_2'(t)$, can be obtained as [22]

$$m_2' = \frac{n \cdot m_1}{n \cdot m_2} m_2.$$

The vector $m_1(t)$ can be computed using (3), and S_1 can be computed as $S_1 = \|m_1 - m_2'\|$. Thus, all three sides of triangle Om_1m_2' are known. Using the properties of similar triangles, between triangles Om_1m_2' and $O\bar{m}_1\bar{m}_2$, and the known length S_1, the vectors $\bar{m}_1(t)$ and $\bar{m}_2(t)$ can be recovered. Solutions for i_x, i_y, and $R(t)$ can now be determined. Since the origin of $\mathcal{F}_c$ is placed at $\bar{m}_1(t)$, the translation is given by $x(t) = \bar{m}_1(t)$. Similarly, the translation $x(t)$ and rotation $R(t)$ can be calculated for every frame.

B. Feedforward Velocity Estimation

A continuous nonlinear estimator is developed in [23] to calculate the linear and angular velocity of a moving object in a stationary camera reference frame. The strategy developed in [23] requires a single known length on the plane and also the rotation matrix R^* between camera frame $\mathcal{F}_c^*$ and initial object reference frame $\mathcal{F}_r$. This nonlinear estimator design is used in the subsequent design. The pose estimation method of Section III-A can be used to compute the rotation matrix R^*. The measurable signals $\bar{R}(t)$, R^*, $\bar{x}(t)$, $d(t)$, d^*, and $\alpha_j(t)$ are available to estimate the velocity. The translation error $e_v(t) \in \mathbb{R}^3$ and rotation error $e_\omega(t) \in \mathbb{R}^3$ given in [30] are quantized as

$$e_v = p_e - p_e^*, \qquad e_\omega = u\theta \tag{5}$$

where $u(t) \in \mathbb{R}^3$ represents a unit rotation axis, $\theta(t) \in \mathbb{R}$ denotes the rotation angle, and $p_e(t)$, $p_e^* \in \mathbb{R}^3$ denote the extended image coordinates as defined in [23].

To achieve the objective of estimating the linear and angular velocity of an object expressed in the camera reference frame and denoted by $V_r(t) = [v_e^T, \omega_e^T]^T \in \mathbb{R}^6$, the error kinematics are expressed as

$$\dot{e} = JV_r \tag{6}$$

where $e(t) \triangleq \begin{bmatrix} e_v & e_\omega \end{bmatrix}^T \in \mathbb{R}^6$ is the error, $J(t) \in \mathbb{R}^{6\times6}$ is a Jacobian-like matrix given by [23]

$$J = \begin{bmatrix} \frac{\alpha_1}{z_1^*} A_e L_v & -\frac{\alpha_1}{z_1^*} A_e L_v R[s_1]_x R^T \\ 0 & L_\omega \end{bmatrix} \tag{7}$$

where $A_e \in \mathbb{R}^{3\times3}$ is a camera calibration matrix, and $L_v(t) \in \mathbb{R}^{3\times3}$ and $L_\omega(t) \in \mathbb{R}^{3\times3}$ are Jacobian-like matrices as defined in [23]. The subsequent development assumes that $V_r(t)$ of (6) is bounded and is second order differentiable with bounded derivatives. It is also assumed that if $V_r(t)$ is bounded, then the structure of (6) ensures that $e(t)$ is bounded.

Let $\hat{e}(t) \in \mathbb{R}^6$ denotes the estimate of the error $e(t)$. An observer $\dot{\hat{e}}(t) \in \mathbb{R}^6$ for $\dot{e}(t)$ is designed as [23]

$$\begin{aligned} \dot{\hat{e}} \;=\; & \int_{t_0}^{t} (K + I_{6\times6})\tilde{e}(\tau)d\tau \\ & + \int_{t_0}^{t} \rho \mathrm{sgn}(\tilde{e}(\tau))d\tau + (K + I_{6\times6})\tilde{e} \end{aligned} \tag{8}$$

where $\tilde{e}(t) \in \mathbb{R}^6 \triangleq e(t) - \hat{e}(t)$ is the estimation error, $K, \rho \in \mathbb{R}^{6\times6}$ are positive definite constant diagonal gain matrices, $I_{6\times6} \in \mathbb{R}^{6\times6}$ denotes the identity matrix, t_0 is the initial time, and the notation $sgn(\tilde{e})$ denotes the standard signum function.

In [23], Lyapunov-based analysis technique are used to show that $\dot{\hat{e}}(t) \to \dot{e}(t)$ as $t \to \infty$, which means $\dot{\hat{e}}(t) \to JV_r$

as $t \to \infty$. Since J is known and invertible, the velocity of an object in the Euclidean frame can be identified as

$$V_r = J^{-1}\dot{\hat{e}}. \tag{9}$$

The position and velocity estimates facilitate the development of a PBVS controller for kinematic control of a UGV. The subsequently designed PBVS controller only uses the velocity in three dimensions, viz.; linear velocity in x-direction and z-direction and angular velocity in y-direction. The following sections describe the kinematic model of the UGV, define the control objective, and show the control development.

IV. Leader-Follower model for UGVs

A. Kinematics of the relative states

The kinematics of the relative states of the UGV formation can be determined as [10]

$$M\begin{bmatrix} \dot{l}_{12} \\ \dot{\psi}_{12} \end{bmatrix} - N\begin{bmatrix} v_1 \\ \omega_1 \end{bmatrix} = \begin{bmatrix} v_2 \\ \omega_2 \end{bmatrix} \tag{10}$$

where the matrices $M(l_{12}, \beta_1) \in \mathbb{R}^{2\times 2}$ and $N(l_{12}, \varphi_{12}, \beta_1) \in \mathbb{R}^{2\times 2}$ are defined as

$$\begin{aligned} M &= \begin{bmatrix} -\cos\beta_1 & -l_{12}\sin\beta_1 \\ (\sin\beta_1)/h & -(l_{12}\cos\beta_1)/h \end{bmatrix}, \\ N &= \begin{bmatrix} -\cos\varphi_{12} & l_{12}\sin\beta_1 \\ -(\sin\varphi_{12})/h & (l_{12}\cos\beta_1)/h \end{bmatrix}. \end{aligned}$$

By defining the relative states vector $q(t) \in \mathbb{R}^2$, as $q = \begin{bmatrix} l_{12} & \psi_{12} \end{bmatrix}^T$, (10) can be expressed in a compact form as

$$M\dot{q} - NV_1 = V_2 \tag{11}$$

where $V_1(t) \in \mathbb{R}^2 = \begin{bmatrix} v_1 & \omega_1 \end{bmatrix}^T$, defines the absolute velocity of the leader UGV, and $V_2(t)$ given by $V_2 \in \mathbb{R}^2 = \begin{bmatrix} v_2 & \omega_2 \end{bmatrix}^T$, defines the absolute velocity of the follower UGV. The motion state of the follower UGV, $V_2(t)$, can be measured using local sensor such as optical encoders mounted on the follower UGV, and $q(t)$ can be calculated using pose reconstruction techniques discussed in Section III-A. The matrices $M(l_{12}, \beta_1)$ and $N(l_{12}, \varphi_{12}, \beta_1)$ can be calculated by using the pose estimates of the leader UGV with respect to the follower UGV, as discussed in Section III-A. The motion state of the leader UGV, $V_1(t)$, is not known directly as no communication is assumed between the UGVs, but can be estimated using the methods in Section III-B.

V. Position-Based Visual Control Development

The contribution of this work is to develop a PBVS control law for controlling the motion of the follower UGV. The subsequently designed controller uses the vision-based relative position and relative velocity estimates of the leader UGV with respect to the follower UGV. The vision-based relative velocity estimation technique is fused with the relative position feedback to achieve the global asymptotic stability for the kinematic control of the non-holonomic UGV. The control law is different from the other leader-follower approaches [11]–[15] in the sense that the designed controller uses the relative pose and the relative velocity of the leader which are estimated using the geometric method and a nonlinear estimator, respectively. The pose and velocity estimation requires only the knowledge of a single length on the leader. The control law does not require the knowledge of the global position of the leader as well as the follower. Also, the control law does not require the global velocity of the leader UGV and does not require it to be a constant. The following section describes the open-loop error system.

A. Control Objective

The PBVS control objective considered here is to design a continuous kinematic controller for the follower UGV to track the motion of the leader UGV. The subsequently designed controller is based on the relative pose and the relative velocity information of the leader UGV, estimated using the camera mounted on the follower UGV. The relative velocity of the follower UGV is measured using local sensors. To quantify the control task in hand, a position tracking error, denoted by $\tilde{q}(t) \in \mathbb{R}^2$ can be expressed as

$$\tilde{q} \triangleq q - q_d \tag{12}$$

where $q_d \in \mathbb{R}^2$ denotes the desired state of the follower UGV with respect to the leader UGV. The control objective dictates that q_d is a constant as it is desired to maintain a constant distance and relative bearing between the leader UGV and the follower UGV.

B. Error System Development

The open-loop tracking error system can be developed, by utilizing the expressions (11) and (12) as

$$\dot{\tilde{q}} = M^{-1}(NV_1 + V_2) \tag{13}$$

where $V_2(t)$, the absolute velocity of the follower UGV, is the control input and $M^{-1}(l_{12}, \beta_1)$ exists $\forall l_{12}(t) \neq 0$. Based on the open-loop error system given by (13), the control input $V_2(t)$ is designed as

$$V_2 = -N\hat{V}_1 - MK_c\tilde{q} \tag{14}$$

where $K_c \in \mathbb{R}^{2\times 2}$ is a control gain matrix. The feedback term consists of the gain matrix multiplied by an error, given by (12). The pose error $\tilde{q}(t)$ can be calculated as the difference between estimated relative pose and desired relative pose of the leader UGV with respect to the follower UGV. The relative pose is estimated as discussed in Section III-A. The feedforward term $\hat{V}_1(t)$ is an estimate of the absolute velocity of the leader in the global reference frame estimated as shown in Section III-B. The closed-loop tracking error can be developed by substituting (14) into (13) as

$$\dot{\tilde{q}} = M^{-1}N\tilde{V}_1 - K_c\tilde{q} \tag{15}$$

where $\tilde{V}_1(t) = V_1 - \hat{V}_1$, is the velocity estimation error. As stated in [23], it can be proved that $\tilde{V}_1(t)$ is uniformly continuous, and $\tilde{V}_1(t) \to 0$ as $t \to \infty$.

C. Stability Analysis

Theorem: Given the closed loop error system in (15), the combined relative velocity feedforward and pose error feedback controller designed as (14) ensures that all the system signals are bounded under closed-loop operation and tracking error is regulated in the sense that

$$\|\tilde{q}(t)\| \to 0 \text{ as } t \to \infty. \tag{16}$$

Proof: Let $V(\tilde{q}, t) \in \mathbb{R}$ be a positive-definite function defined as

$$V(t) \triangleq \frac{1}{2}\tilde{q}^T\tilde{q}. \tag{17}$$

After using the closed-loop error (15), the time derivative of $V(t)$ can be expressed as

$$\dot{V} \leq -k\tilde{q}^T\tilde{q} + \tilde{q}^T M^{-1} N \tilde{V}_1. \tag{18}$$

where $k = \lambda_{\max}\{K_c\} \in \mathbb{R}$ where $\lambda_{\max}\{\cdot\}$ denotes the maximum Eigenvalue of the argument. Since the second term in (18) can be proven to be uniformly continuous, the fact that

$$\tilde{V}_1 \to 0 \text{ as } t \to \infty,$$

can be used along with Extended Barbalat's Lemma [31] to conclude that $\tilde{q}(t), \dot{V}(t) \to 0$ as $t \to \infty$.

VI. Simulation Results

The controller developed in Section V was implemented in C++. The leader UGV trajectory was generated using a constant linear velocity in z-direction and angular velocity about y-direction using the function $A(1 - \sin(4\pi t))$. The linear and the angular velocities about other axes were zero. The initial positions of the leader and the follower were set to $\begin{bmatrix} 0 & 0 & 100 \end{bmatrix}^T m$ and $\begin{bmatrix} 0 & 0 & 10 \end{bmatrix}^T m$, respectively in the global reference frame. The initial orientation of the leader and the follower was zero radians in global reference frame. The initial velocities of the leader and follower were set zero. Four feature points were fixed on the leader UGV, whose location is known in the leader reference frame. The feature points were tracked throughout the simulation. The relative pose (i.e. translation and rotation) of leader was reconstructed with respect to the follower in the follower reference frame using the pose estimation method described in Section III-A. The relative velocity of the leader was computed using the nonlinear estimator discussed in Section III-B. The desired relative states between the leader and the follower, i.e. the desired relative position, $l_{12}(t)$ and relative orientation, $\psi_{12}(t)$ between the leader and the follower were $l_{12} = 7m$ and $\psi_{12} = 3.14rad$. The trajectories of the leader and the follower are shown in the Fig. 4. The velocity estimator gains were chosen as $K = \begin{bmatrix} 300 & 300 & 200 & 15 & 15 & 15 \end{bmatrix} \times 10^{-5}$ and $\rho = \begin{bmatrix} 100 & 100 & 10 & 10 & 1 & 1 \end{bmatrix} \times 10^{-7}$. The follower control parameters were chosen upon trial and error

$$K_c = \begin{bmatrix} 2 & 0 \\ 0 & 1 \end{bmatrix}.$$

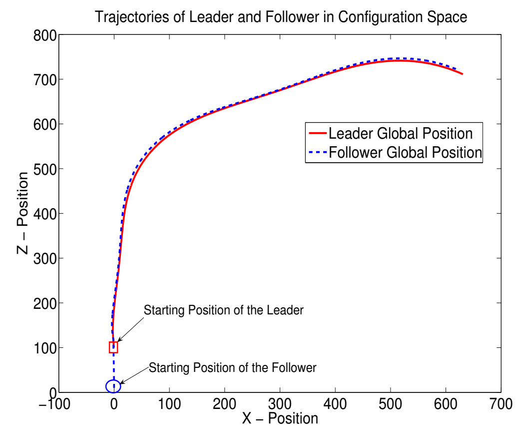

Fig. 4. Trajectory of the leader and the follower

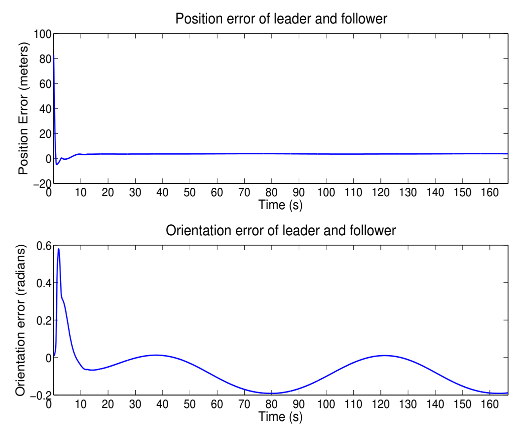

Fig. 5. The position and orientation error

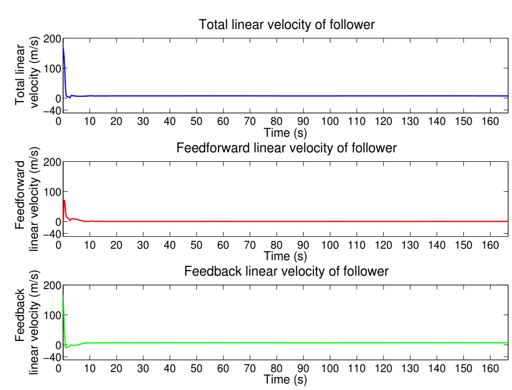

Fig. 6. Follower linear velocity control input

The evolution of the position and orientation errors can be seen Fig. 5. From Fig. 6, the observation can be made that input velocity of the follower is bounded. Velocity estimator takes some time to converge to *true* value of the relative velocity of the leader and initially the error is high. Thus, initially the feedback part of the controller puts in more efforts and feedforward part does not have significant contribution. As the velocity estimates converge to true value, it can be observed from Fig. 6, that control input is dominated by feedforward part. Observations can be extended from Fig. 6 to see that as the follower achieves the velocities of the leader, i.e. feedforward term tends to zero and control input is solely guided by the position error.

VII. Conclusion And Future Work

In this paper, a PBVS strategy is presented to address the problem of leader-follower formation control. The proposed controller uses vision-based estimation methods to estimate the relative position, relative orientation and relative velocity of the leader with respect to the follower in the follower reference frame. This eliminates the requirement of knowledge of the position and velocity of the leader and follower in the global reference frame. Thus, the proposed control strategy can work with only a single camera mounted on the follower UGV. The position error is fed back along with feedforward relative velocity, which adds more kinematic knowledge to the controller about the leader with respect to the follower. Global asymptotic stability is ensured for tracking the leader using the proposed control law.

Future efforts will focus on eliminating the need for the knowledge of single length on the leader. Also, the dynamics of the follower will be considered to achieve a more realistic control.

References

[1] T. Balch and R. Arkin, "Behavior-based formation control for multirobot teams," *IEEE Transactions on Robotics and Automation*, vol. 14, no. 6, pp. 926–939, Dec 1998.

[2] L. E. Parker, "Current state of the art in distributed autonomous mobile robotics," in *Distributed Autonomous Robotic Systems*. Springer, 2000, pp. 3–12.

[3] J. Desai, J. Ostrowski, and V. Kumar, "Modeling and control of formations of nonholonomic mobile robots," *IEEE Transactions on Robotics and Automation*, vol. 17, no. 6, pp. 905–908, 2001.

[4] G. Antonelli and S. Chiaverini, "Kinematic control of platoons of autonomous vehicles," *IEEE Transactions on Robotics*, vol. 22, no. 22, pp. 1285–1292, Dec 2006.

[5] T. Balch and R. Arkin, "Behavior-based Formation Control for Multirobot," *IEEE Transactions on Robotics and Automation*, vol. 14, pp. 926–939, 1998.

[6] S. Monteiro and E. Bicho, "A dynamical systems approach to behavior-based formation control," in *Proc. of IEEE International Conference on Robotics and Automation*, vol. 3, Washington, DC, May 2002, pp. 2606–2611.

[7] M. Lewis and K. Tan, "High Precision Formation Control of Mobile Robots Using Virtual Structures," *Autonomous Robots*, vol. 4, no. 4, pp. 387–403, 1997.

[8] D. Swaroop and J. Hedrick, "String stability of interconnected systems," *IEEE Transactions on Automatic Control*, vol. 41, no. 3, pp. 349–357, Mar 1996.

[9] X. Chen, A. Serrani, and H. Ozbay, "Control of leader-follower formations of terrestrial uavs," in *Proc. of IEEE Conference on Decision and Control*, vol. 1, Maui, Hawaii, Dec. 2003, pp. 498–503.

[10] S. Liu, D. Tan, and G. Liu, "Robust leader-follower formation control of mobile robots based on a second order kinematics model," *Acta Automatica Sinica*, vol. 33, no. 9, pp. 947–955, 2007.

[11] A. Das, R. Fierro, V. Kumar, J. Ostrowski, J. Spletzer, and C. Taylor, "A vision-based formation control framework," *IEEE Transactions on Robotics and Automation*, vol. 18, no. 5, pp. 813–825, 2002.

[12] R. Vidal, O. Shakernia, and S. Sastry, "Omnidirectional vision-based formation control," in *Proc of Annual Allerton Conference on Communication Control and Computing*, vol. 40, no. 3. The University; 1998, 2002, pp. 1638–1647.

[13] H. Kannan, V. Chitrakaran, D. Dawson, and T. Burg, "Vision-Based Leader/Follower Tracking for Nonholonomic Mobile Robots," in *American Control Conference, 2007*, New York City, July 2007, pp. 2159–2164.

[14] S. Benhimane, E. Malis, P. Rives, and J. Azinheira, "Vision-based control for car platooning using homography decomposition," in *Proc. IEEE Int. Conf. Robotics and Automation*, April 2005, pp. 2161–2166.

[15] E. Johnson, A. Calise, R. Sattigeri, Y. Watanabe, and V. Madyastha, "Approaches to Vision-Based Formation Control," in *IEEE Conference on Decision and Control*, Atlantis, Paradise Island, Bahamas, Dec 2004.

[16] S. Hutchinson, G. Hager, and P. Corke, "A tutorial on visual servo control," *IEEE Trans. Robot. Automat.*, vol. 12, no. 5, pp. 651–670, Oct. 1996.

[17] B. Espiau, F. Chaumette, and P. Rives, "A new approach to visual servoing in robotics," *IEEE Trans. Robot. Automat.*, vol. 8, no. 3, pp. 313–326, June 1992.

[18] P. Martinet, J. Gallice, and D. Khadraoui, "Vision based control law using 3D visual features," in *Proc. WAC 96*, vol. 3, 1996, pp. 497–502.

[19] R. Hartley, "In defence of the eight-point algorithm," *IEEE Trans. Pattern Anal. Machine Intell.*, vol. 19, pp. 580–593, 1997.

[20] O. D. Faugeras and F. Lustman, "Motion and structure from motion in a piecewise planar environment," *Int. J. Pattern Recog. and Artificial Intell.*, vol. 2, no. 3, pp. 485–508, 1988.

[21] D. DeMenthon and L. S. Davis, "Model-based object pose in 25 lines code," in *European Conf. on Computer Vision*, 1992, pp. 335–343.

[22] N. Gans, A. P. Dani, and W. E. Dixon, "Visual servoing to an arbitrary pose with respect to an object given a single known length," in *Proceedings of the 2008 American Control Conference*, Seattle, WA, June 2008, pp. 1261–1267.

[23] V. Chitrakaran, D. M. Dawson, W. E. Dixon, and J. Chen, "Identification a moving object´s velocity with a fixed camera," *Automatica*, vol. 41, no. 3, pp. 553–562, 2005.

[24] A. P. Dani, S. Velat, C. Crane, N. Gans, and W. E. Dixon, "Experimental results of image-based pose and velocity estimation," in *Proc. of IEEE Multi-Conference on Systems and Control*, San Antonio, TX, Sept. 2008, pp. 1159–1164.

[25] A. Das, R. Fierro, V. Kumar, B. Southall, J. Spletzer, and C. Taylor, "Real-time vision-based control of a nonholonomic mobile robot," in *Proceedings of IEEE International Conference on Robotics and Automation*, vol. 2, Seoul, Korea, May 2001, pp. 1714– 1719.

[26] O. Orqueda and R. Fierro, "Robust vision-based nonlinear formation control," in *Proc. American Control Conference*, June 2006, pp. 1422–1427.

[27] R. DeSantis, E. Polytech, and Q. Montreal, "Path-tracking for car-like robots with single and double steering," *IEEE Transactions on Vehicular Technology*, vol. 44, no. 2, pp. 366–377, 1995.

[28] Z. Zhang and A. Hanson, "3D reconstruction based on homography mapping," in *Proc. ARPA Image Understanding Workshop Palm Springs CA*, 1996.

[29] Y. Ma, S. Soatto, J. Kosecká, and S. Sastry, *An Invitation to 3-D Vision*. Springer, 2004.

[30] M. Spong, M. W. & Vidyasagar, *Robot Dynamics and Control*. New York: Wiley, 1989.

[31] W. E. Dixon, D. M. Dawson, E. Zergeroglu, and A. Bahal, *Nonlinear Control of Wheeled Mobile Robots*. Springer, 2001.